A Method for the Computation of the Characteristic Immittance Matrix of Multiconductor Striplines with Arbitrary Widths

L. J. PETER LINNÉR, MEMBER, IEEE

Abstract—**An exact method for the computation of the characteristic impedance matrix of coplanar coupled multiconductor striplines with arbitrary widths is presented. The system of conductors is enclosed in a rectangular shielding box with a homogeneous dielectric medium. Use is made of conformal mapping by hyperelliptic integrals. The reverse problem of determining the geometrical dimensions for a given characteristic impedance matrix is solved by employing an optimization procedure in conjunction with carefully determined initial approximations. This yields low computer running time compared to current methods for the treatment of multiconductor transmission lines.**

I. INTRODUCTION

THE PROBLEM of determining the characteristic impedance parameters of transmission lines has been of great interest for a long time; in the beginning, chiefly from a mathematical–physical standpoint. In [1] many of these earlier works have been collected. Mostly, the approach taken has been to consider the existence of (quasi-) TEM modes only, thereby transforming the problem to that of determining Maxwell's capacitance matrix of the conductors for a two-dimensional static electrical potential problem. In the next step one can proceed in several ways as follows. 1) Solve the Laplace equation in the region of interest, either exactly with orthogonal polynomial expansions, or with finite difference methods. 2) Use the conformal mapping technique to transform into a structure with known properties. 3) Solve integral equations derived from Green functions, to mention the most common methods.

A multitude of different methods under 1)–3) mentioned previously is available for single or multiple conductor transmission lines. The dielectric filling between the conductors may be homogeneous or not. Below, the restricted problem of multiple-strip transmission lines between parallel ground planes and with homogeneous dielectric will be treated, although extensions that approximate inhomogeneous cases can be made, for instance, as in [2].

In 1943 Magnus and Oberhettinger [3] presented several new practical single-strip transmission lines with exact formulas for the characteristic impedance. The single-strip conductor with zero thickness symmetrically placed between two parallel ground planes with and without walls was treated. Later, Cohn [4] gave graphs and correction formulas for the second case with a nonzero-strip thickness. Exact formulas were provided by Bates [5]. Other works on single-strip transmission lines can be found in [6]–[9].

By introducing the even and odd wave impedances Cohn succeeded in arriving at exact formulas and versatile nomograms for the analysis of the symmetrical coupled two-strip transmission line between parallel ground planes [10]. Also, he included correction formulas for nonzero thickness. Ekinge [8] gives formulas in the case when the symmetrical two-strip conductor is surrounded by a shielding rectangular box. The symmetrical case has also been treated in [6] and [9]. The nonsymmetrical case in which the two coupled strips are of different widths has been given some attention with the previously mentioned methods 1) as well as 2) in an approximate manner [9], [11]–[13]. However, the results obtained differ considerably. This case (with side walls as well) will be included in the exact analysis which follows.

Multiple-strip transmission lines with more than two inner conductors have been treated before to some extent. Thus Itakura *et al.* [14] have derived exact formulas for the case with three conductors with equal-width outer conductors and conductor spacings. General N-strip transmission lines have been approximately analyzed by considering the different conductors as a number of pairs of coupled conductors by methods such as [8] and [10]. In case of equal widths and spacings of the conductors there exists an extension of the method in [10] also used in [14], whereby an infinite array of conductors is considered. The reasoning is as follows. The conductors are given equal potentials with opposite signs periodically repeated along the array. By combining such different modes it follows from superposition that nonadjacent conductors can be given opposing potentials and the conductors in between the potential zero. This was first shown by Dunn [15] and later transferred to the case with the equal-width equal-spacing strip conductors on the line of symmetry between the two parallel ground planes [16] and [17]. Lennartsson [18] has presented a network analogue method for the solutions of the two-dimensional Laplace's equation. Three-conductor systems in a stratified dielectric within a surrounding rectangular box can be readily analyzed on a computer at the expense of time consumption and lack of direct error control. An additional feature of this method is that conductors situated on separated parallel lines can be treated.

In the following, an exact analysis of a multiple-conductor strip transmission line placed symmetrically between two parallel ground planes with or without side walls

Manuscript received March 7, 1974; revised July 5, 1974.
The author was with the Division of Network Theory, Chalmers University of Technology, Gothenburg, Sweden. He is now with the MI-Division, Telefonaktiebolaget L M Ericsson, Mölndal, Sweden.

will be given. The conductor widths and the spacings in between can be assigned arbitrarily.

II. CONFORMAL MAPPING BY SCHWARZ–CHRISTOFFEL TRANSFORMATIONS

The conformal mapping technique has been applied to a variety of problems in engineering and physics. The invariant property of the Laplace equation under such a transformation makes it possible to transform the problem to a (simpler) geometry, where a solution is available or can be readily found. This technique will be used below as well.

The basic problem connected with characteristic impedance analysis is that the region to be mapped is multiply connected. This has been avoided by considering symmetrical geometries only. In such cases the mapping of a subregion with the conductors on the boundary is possible. This is the starting point of the theory.

Consider a multiple-conductor stripline between two parallel ground planes, Fig. 1. Here the widths and spacings of the n inner conductors can be chosen arbitrarily. The dielectric constant of the homogeneous medium is ϵ_r and the case with no side walls can be treated by setting $d = \infty$. The upper half-plane part of the rectangular box can now be mapped into the entire upper half-plane in Fig. 2 by a Schwarz–Christoffel transformation. This can be conveniently expressed in Jabobi's elliptic functions as given by

$$y = sn\left[2\frac{K'(k)}{b}x, k\right] \tag{1}$$

where

$$k = \left[\frac{\nu_2(0 \mid i\lambda)}{\nu_3(0 \mid i\lambda)}\right]^2$$

and

$$K'[k(\lambda)] = \frac{\pi}{2}\nu_3^2\left(0 \mid i\frac{1}{\lambda}\right)$$

with

$$\lambda = b/d \quad \text{and} \quad i = (-1)^{1/2}.$$

This is clear from [19] and [3] when considering the module equation

$$\frac{K'(k)}{K(k)} = \frac{b}{d}. \tag{2}$$

Here K is the complete elliptic function of the first kind, and $\nu_j(0)$ are Jacobi's theta functions as given in [20]. The configuration with no side walls, $d = \infty$, can be obtained from (1) as a limiting case:

$$y = \tanh(\pi x/b) \qquad (d = \infty). \tag{1a}$$

It deserves mentioning that the use of Jacobi's theta functions facilitates the numerical computations considerably [19].

In the next step we look for a mapping function which transforms the y plane in such a way that a homogeneous field is obtained when a certain voltage distribution is applied to the n inner conductors. This is again achieved by a Schwarz–Christoffel transformation. The final configuration with the required properties is shown in Fig. 3. The mapping function is given by

$$\frac{dz}{dy} = \prod_{m=1;\, m\neq k}^{n}(y - y_{0m}) \Big/ \prod_{m=1}^{2n+2}(y - y_m)^{1/2} \tag{3}$$

where each of the numerator factors accounts for 180° bends at $n - 1$ of the conductors in Fig. 3. There are n such mappings with the kth conductor unfolded. A homogeneous electric field is now obtained for any voltage applied to conductor k with the remaining conductors left on floating potentials. This is obvious from the boundary conditions on the side walls: $\partial\phi/\partial n = 0$.

The geometrical dimensions of Fig. 3 are given by definite integrals of (3). However, the numerator polynomial roots of the integrand are not given explicitly. To determine the numerator polynomial consider the following kind of integrals:

$$F_{ij} = \int_{y_{2i}}^{y_{2i+1}} [y^{j-1} \Big/ \prod_{m=1}^{2n+2}(y - y_m)^{1/2}]\, dy \tag{4}$$

where the path of integration is along the ith conductor in Fig. 2. From Fig. 3 it appears that the total integral must equal zero:

$$\sum_{j=1}^{n} a_j F_{ij} = 0, \qquad (i \neq k) \tag{5}$$

for all conductors but the kth one because $z_{2i} = z_{2i+1}$. Rather than try to solve for the polynomial roots of the numerator in (3) the corresponding coefficients a_j have been introduced. Thus the polynomial coefficients are determined from

$$\boldsymbol{F}_k\boldsymbol{a}_k = \boldsymbol{0}, \qquad (k = 1 \rightarrow n) \tag{6}$$

for each conductor k unfolded. Here $\boldsymbol{F}_k$ is an $(n - 1) \times n$ matrix obtained when the kth row is deleted from the

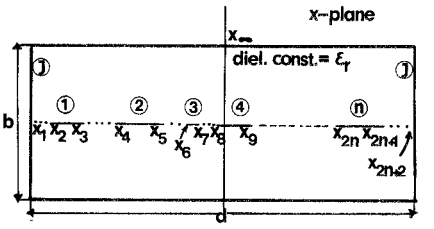

Fig. 1. The multiconductor stripline surrounded by a rectangular shield.

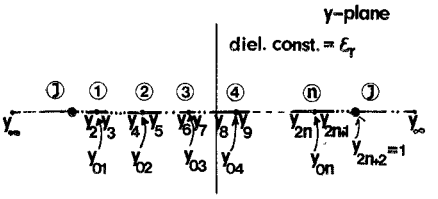

Fig. 2. The intermediate mapping step.

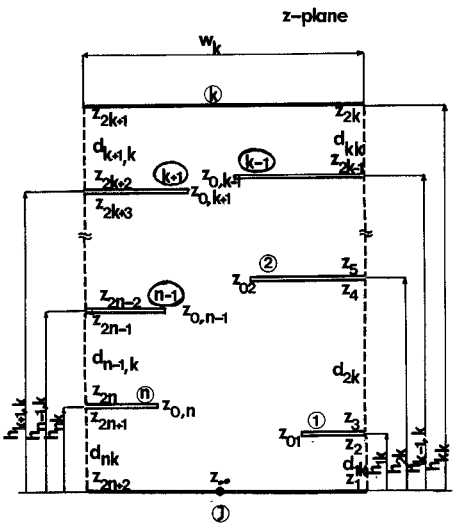

Fig. 3. The final mapping step where the field can be made homogeneous for certain conductor potentials.

matrix

$$\boldsymbol{F} = \begin{bmatrix} F_{11} & F_{12} & \cdots & F_{1n} \\ F_{21} & F_{22} & & \\ \cdot & & \cdot & \\ \cdot & & & \cdot \\ \cdot & & & \\ F_{n1} & & & F_{nn} \end{bmatrix}.$$

The matrix elements are determined by (4). The polynomial coefficients are given by the column vector

$$\boldsymbol{a}_k = [a_{k1}, a_{k2}, \cdots a_{kn}]^T$$

with its first element arbitrarily chosen equal to unity.

Now, consider the integrals

$$G_{ij} = \frac{1}{(-1)^{1/2}} \int_{y_{2i-1}}^{y_{2i}} \left[y^{j-1} / \prod_{m=1}^{2n+2} (y - y_m)^{1/2} \right] dy. \quad (7)$$

To obtain the distances between consecutive conductors along the magnetic walls of Fig. 3, sums of the following kind must be computed:

$$\sum_{j=1}^{n} a_j G_{ij}. \quad (8)$$

Next, the distance column vector

$$\boldsymbol{d}_k = [d_{1k}, d_{2k}, \cdots d_{n+1,k}]^T$$

with its elements given in Fig. 3 is computed from

$$\boldsymbol{d}_k = \boldsymbol{G}\boldsymbol{a}_k \quad (9)$$

where

$$\boldsymbol{G} = \begin{bmatrix} G_{11} & G_{12} & \cdots & G_{1n} \\ G_{21} & G_{22} & & \\ \cdot & & \cdot & \\ \cdot & & & \cdot \\ \cdot & & & \\ G_{n+1,1} & & & G_{n+1,n} \end{bmatrix}$$

and the elements are given by (7). From $\boldsymbol{d}_k$, the distances between the different conductors and the ground conductors,

$$\boldsymbol{h}_k = [h_{1k}, h_{2k}, \cdots h_{nk}]^T$$

are easily determined. Finally, the length of the kth unfolded conductor in Fig. 3 w_k is given by

$$w_k = \boldsymbol{f}_k^T \boldsymbol{a}_k \quad (10)$$

where $\boldsymbol{f}_k^T$ is the kth row of $\boldsymbol{F}$. The integrals in (4) and (7) appear to be improper with the integrand behaving singularly at the endpoints. The analytical and numerical aspects of such integrals are discussed in the Appendix.

III. THE DETERMINATION OF THE CHARACTERISTIC IMMITTANCE MATRIX

The configuration of Fig. 3 can now be used to determine the characteristic impedance matrix

$$\boldsymbol{Z}_0 = \begin{bmatrix} z_{11} & z_{12} & \cdots & z_{1n} \\ z_{21} & z_{22} & & \\ \cdot & & \cdot & \\ \cdot & & & \cdot \\ \cdot & & & \\ z_{n1} & & & z_{nn} \end{bmatrix}. \quad (11)$$

To do this consider the Maxwell's per-unit length capacitance matrix of the n-conductor system [Fig. 4(a)]:

$$\boldsymbol{C} = \begin{bmatrix} c_{11} & -c_{12} & \cdots & -c_{1n} \\ -c_{21} & c_{22} & & \\ \cdot & & \cdot & \\ \cdot & & & \cdot \\ \cdot & & & \\ -c_{n1} & & & c_{nn} \end{bmatrix} \quad (12)$$

where $c_{ii} = c_i + \sum_{j=1;\, j\neq i}^{n} c_{ij}$. (13)

This matrix is related to $\boldsymbol{Y}_0 = \boldsymbol{Z}_0^{-1}$ by the relation $\boldsymbol{Y}_0 = v\boldsymbol{C}$, where $v = c_0/(\epsilon_r)^{1/2}$ is light's velocity in the dielectric medium while c_0 is the velocity of light in vacuum. Now, apply a unit dc voltage between conductor k and the ground J, with the remaining conductors left with floating potentials in Fig. 3. It is clear from the previous discussion that the electric field is homogeneous and that the paths of constant potentials parallel all conductor surfaces. Thus every conductor takes a potential that is proportional to its height above the ground conductor J. To compute the elements of $\boldsymbol{Z}_0$ consider (11) as representing a resistive n-port Fig. 4(b), each port with the ground and the corresponding conductor as terminals. From the definition of the z parameters we have

$$z_{lk} = \left. \frac{V_l}{I_k} \right|_{I_j = 0;\, j \neq k}. \quad (14)$$

V_l and I_k represent the voltage and current at the lth and kth ports, respectively. Returning to Fig. 3, this is

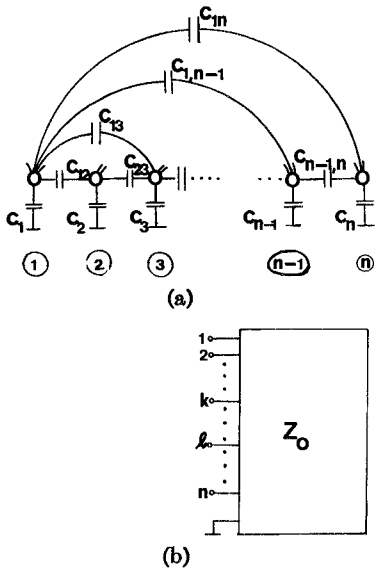

Fig. 4. (a) The per-unit length capacitances of a general n-conductor transmission line. (b) Its characteristic impedance matrix $\boldsymbol{Z}_0$ representing a resistive n port.

exactly the condition to which we are confined with the electric field in Fig. 3 kept homogeneous. Thus we have for the diagonal elements of (11):

$$2z_{kk} = \left(\frac{\mu_0}{\epsilon_r\epsilon_0}\right)^{1/2} \frac{h_{kk}}{w_k}. \tag{15}$$

The factor 2 arises from the fact that the conformal mapping is applied to the upper half-space of Fig. 2.

The off-diagonal elements can be computed as follows, recognizing the n-port voltage transfer function:

$$\alpha_{lk} = \left.\frac{V_l}{I_k}\right|_{I_j=0;\, j\neq k} = \frac{z_{lk}}{z_{kk}} \tag{16}$$

from elementary network theory. But Fig. 3 yields

$$\alpha_{lk} = \frac{h_{lk}}{h_{kk}}. \tag{17}$$

Thus

$$2z_{lk} = \left(\frac{\mu_0}{\epsilon_r\epsilon_0}\right)^{1/2} \frac{h_{lk}}{w_k}. \tag{18}$$

The complete characteristic impedance matrix is now given by

$$\boldsymbol{Z}_0 = \frac{Z_0}{2(\epsilon_r)^{1/2}} \begin{pmatrix} \frac{h_{11}}{w_1} & \frac{h_{12}}{w_2} & \cdots & \frac{h_{1n}}{w_n} \\ \frac{h_{21}}{w_1} & \frac{h_{22}}{w_2} & & \\ \vdots & \vdots & \ddots & \\ \frac{h_{n1}}{w_1} & \frac{h_{n2}}{w_2} & & \frac{h_{nn}}{w_n} \end{pmatrix} \tag{19}$$

where the free space characteristic impedance $Z_0 = (\mu_0/\epsilon_r)^{1/2}$ has been used. A simple inversion of (19) yields the characteristic admittance matrix $\boldsymbol{Y}_0$.

The computational efforts can be decreased by observing the fact that characteristic immittance matrices are symmetrical. The number of definite integrals to be evaluated therefore decreases from $n(2n+1)$ to $n(3n+1)/2$.

IV. THE SYNTHESIS PROBLEM

So far, we have been concerned with the problem of determining the characteristic immittance matrix for a given structure, i.e., characteristic immittance analysis. In practical design the reverse problem of determining the structure for a given characteristic immittance matrix, i.e., wave immittance synthesis, is of predominant interest. The sparse treatment of hyperelliptic integrals in the literature [4], [7] makes it still more difficult to find their inverse functions. Thus in the synthesis the mapping from Fig. 3 to Fig. 2 must be done by some type of optimization procedure employing a repeated mapping from Fig. 2 to Fig. 3, while the mapping from Fig. 2 to Fig. 1 can be performed with the inverse function of (1):

$$x = \frac{b}{2K'(k)} F(\arcsin y, k) \tag{20}$$

where F is the normal elliptic integral of the first kind. In the synthesis procedure used, the independent variable vector is $[y_2, y_3, \cdots y_{2n}]^T$. The objective function is the summed squared difference of elements between the characteristic admittance matrix wanted and that obtained from the optimization procedure. Counting the number of variables involved we obtain $2n-1$ and $n(n+1)/2$, respectively, for the symmetrical matrix. To deal with a well-determined problem only $2n-1$ elements of the characteristic admittance matrix can be used in the optimization. The most rational choice is the main diagonal and the first offset diagonal corresponding to the conductor shield and the neighboring conductor–conductor characteristic admittances, these being the dominant quantities. The reason for using only $2n-1$ out of $2n$ variables in Fig. 2 is their inherent functional dependence. To show this, employ the following bilinear transformation which keeps -1 and $+1$ as fixed points:

$$y' = \frac{y+\alpha}{\alpha y + 1}. \tag{21}$$

It is now easy to show that a suitable transformation always yields the constraint $y_2' = -y_{2n-1}'$ from a choice of

$$\alpha = \{[(1-y_2^2)(1-y_{2n+1}^2)]^{1/2} - (1 + y_2 y_{2n+1})\}/(y_2 + y_{2n+1}). \tag{22}$$

Thus there are only $2n-1$ independent variables. Still more features can be drawn from (21). Obviously, the transformation is an analytical mapping that keeps the characteristic immittance properties invariant. In the synthesis case we can use the mapping of (21) on the Fig. 2 structure obtained to alter the conductor positions of the final structure of Fig. 1. For example, a certain

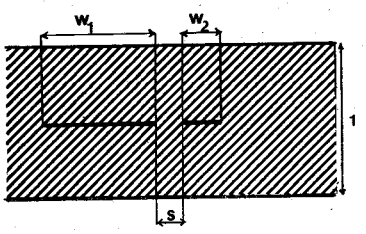

(a)

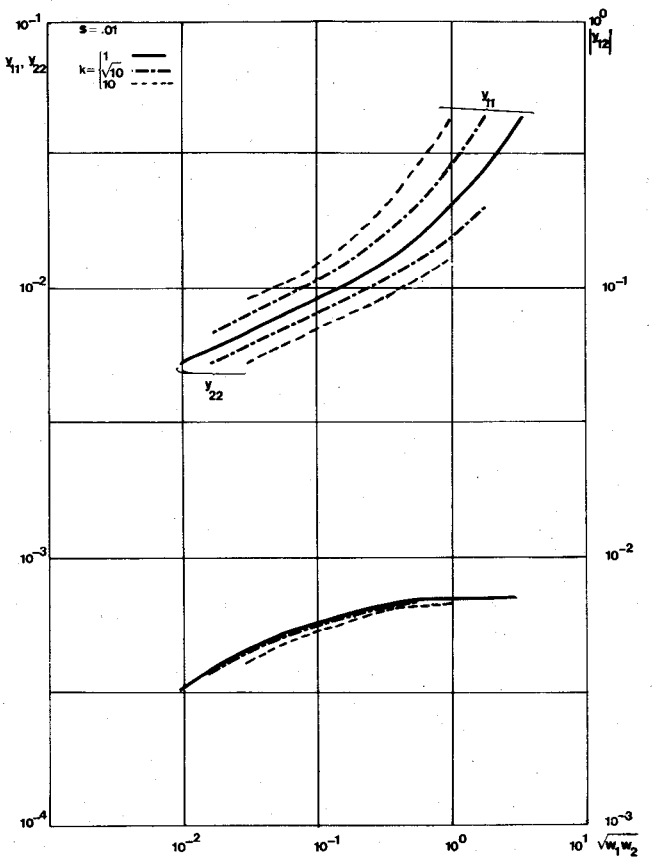

(b)

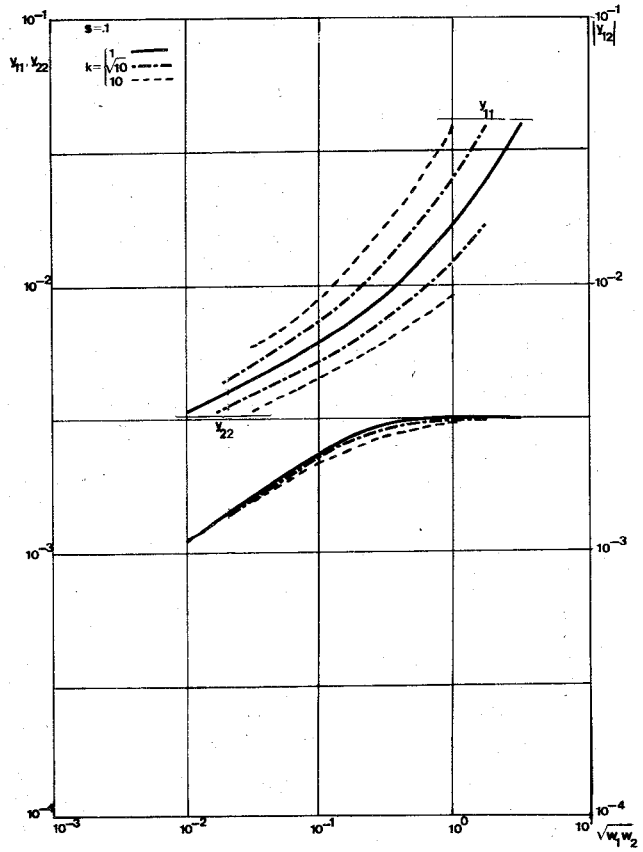

(c)

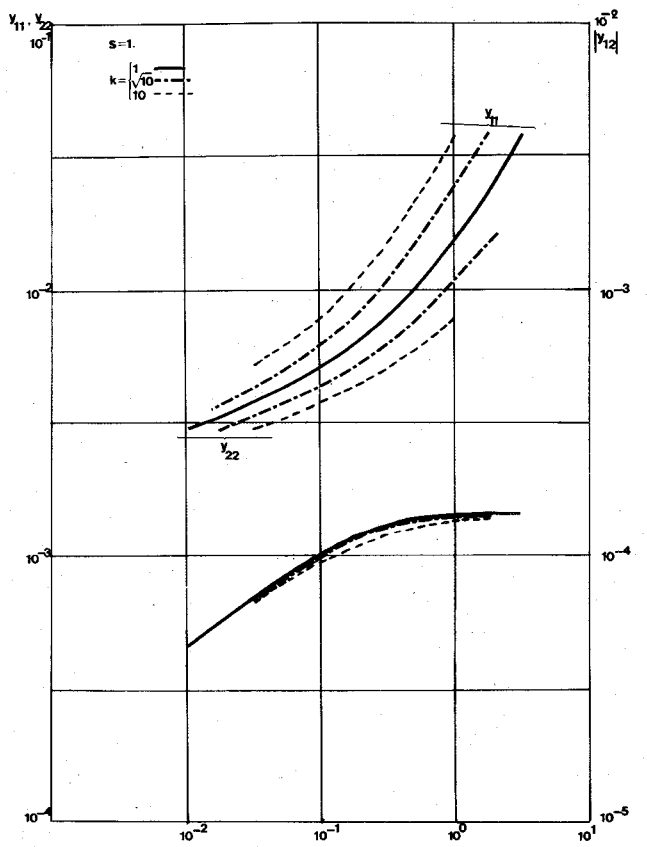

(d)

Fig. 5. (a) The nonsymmetrically coupled transmission lines. (b)–(d) Some characteristic admittance matrix data for different geometrical dimensions.

TABLE I
COMPARISON BETWEEN THE EXACT ANALYSIS AND THE APPROXIMATION WITH COHN'S METHOD APPLIED TO THE NONSYMMETRICAL COUPLED TWO-WIRE TRANSMISSION LINE

$w_2 = kw_1$	Refer to Fig.5(a)	Deviation in percent ($y_{11}/y_{22}/-y_{12}$)		
k	w_1	s = .01	s = .1	s = 1.
$\sqrt{10}$	.01	-4.0/+5.7/+3.0	-1.6/+2.2/+0.13	+0.10/+0.13/-0.14
	.1	-0.62/+0.84/+2.2	-0.42/+0.54/+2.9	+0.08/-0.02/+2.6
	1.	+0.07/-2.7/+0.09	+0.07/-0.02/+0.11	+0.07/-0.03/+0.12
10	.01	-5.4/+9.8/+9.4	-2.8/+4.1/+2.9	+0.09/+0.12/+0.01
	.1	-0.62/+0.56/+6.9	-0.49/+0.31/+10.5	+0.07/-0.03/+11.5

conductor can always be placed anywhere on the line of symmetry, or the conductors as a whole can be centered to minimize the effects of the side walls. Of course, the shape of the box can be arbitrarily changed in this step. This flexibility obliterates the need to resynthesize a given characteristic immittance matrix for different geometrical structures.

For a useful synthesis procedure an effective optimization procedure is not sufficient in terms of the number of iterations needed, i.e., computer time and cost. It is also important to support the synthesis procedure with a sufficiently good starting approximation in Fig. 2 as close as possible to the correct solution point in the $(2n-1)$-dimensional space. This is achieved with the use of a modified Cohn procedure on consecutive pairs of conductors in Fig. 1 with no side walls employed. This is outlined in Section V. The latter condition is necessary to obtain a good starting approximation and implies no condition whether to use side walls or not in the finally synthesized structure of Fig. 1. The optimization procedure being employed in the synthesis procedure is a transitional Newton iteration/steepest descent algorithm with internal computation of the Jacobian. This algorithm is due to Powell [21].

V. RESULTS AND DISCUSSIONS

The method just mentioned has been programmed and run on an IBM 360/65 for some time. Because of the automatic quadrature algorithm employed, which is mentioned in the Appendix, it is possible to require an analysis to be correct to a certain number of digits, thereby reducing the computer time considerably for different applications. The method has been checked against Cohn's method [10] and Ekinge's rectangular box treatment [8] which are exact in the case of two coupled symmetrical conductors. No deviation in the first five digits of the solution has been discovered. In the case of nonsymmetrical coupled conductors, as in Fig. 5(a), some data have been collected in Fig. 5(b)–(d). The characteristic admittance for a configuration given by Fig. 5(a) has been computed varying the distance between the conductors, the width ratio, and the geometrical mean width. From the diagrams it is observed that the conductor–conductor characteristic admittance $|y_{12}|$ as expected only varies slightly for a fixed conductor spacing and geometrical mean width. The deviation is smaller than 6 and 12 percent for $w_1/w_2 = (10)^{1/2}$ and 10, respectively. These percentages also give an indication of the errors in approximately computing the conductor spacings from the inverse of Cohn's method [19] considering

$$y_{11}' = y_{22}' = (y_{11}y_{22})^{1/2} \quad \text{and} \quad w_1' = w_2' = (w_1w_2)^{1/2}.$$

Similarly, the widths can be computed with

$$y_{11}'' = y_{22}'' = y_{ii} \quad \text{and} \quad w_1'' = w_2'' = w_i, \qquad (i = 1,2).$$

The resulting errors are shown in Table I for some cases.

The use of diagrams in finding the geometrical dimensions is not convenient because of the many parameters involved. A user-oriented computer program is far more flexible and is necessary for cases with more than two coupled conductors. Some results from such cases are shown in Table II, where they are compared with data from earlier works by Kollberg [16]. It is shown how the new method can be applied with an increasing number of conductors to yield the characteristic coupling admittances for an infinite array as a limit value. From Table II it is obvious that a very good approximation of the limit value is obtained as soon as the number of conductors is great enough to prevent the two coupling conductors from being the outer ones. Also the table gives an indication of the error involved using the approximate method of Kollberg [16].

The computer running time in cases of analysis is less than 1 and 2 s for two and three coupled conductors, respectively, with a required accuracy of three digits in the result. For a constant accuracy the running time is roughly increasing with n^2, where n is the number of conductors. The synthesis procedure takes the same time of analysis for each step of iteration in the optimization algorithm. The number of iterations increases as $\sim n^2$ for multiple conductor systems.

It is also worth mentioning that the method given here is applicable to any n-conductor problem that can be conformally mapped on Fig. 2. The most immediate structures to extend the method to are those similar to those previously mentioned, but with finite thickness. Obviously, hyperelliptic mapping functions similar to those used here can be employed in transforming from Fig. 2 to the thick-conductor structure. However, additional optimization techniques must be used for such structures.

TABLE II

CHARACTERISTIC ADMITTANCE PARAMETERS FOR MULTICONDUCTOR TRANSMISSION LINES WITH EQUAL WIDTHS AND SPACINGS

Refer to Fig. 1	w = .1875, s = .625				w = .625, s = .1875				w = 1.05, s = .35		
n	3	4	5	∞,[16]	3	4	5	∞,[16]	3	4	∞,[16]
y_{11}	1.713	1.714	1.714	1.928	2.840	2.841	2.841	3.598	5.644	5.644	6.095
y_{22}	1.824	1.827	1.828	1.928	3.387	3.391	3.393	3.598	5.714	5.714	6.095
y_{33}	1.713	1.827	1.830	1.928	2.840	3.391	3.396	3.598	5.644	5.714	6.095
$-y_{12}$	.4372	.4363	.4363	.442	1.168	1.167	1.167	1.200	.4117	.4117	.4375
$-y_{23}$	.4372	.4172	.4153	.442	1.168	1.126	1.125	1.200	.4117	.4117	.4375
$-y_{13}$	8.24-2	7.74-2	7.73-2	7.25-2	.106	9.78-2	9.76-2	9.00-2	8.99-5	8.99-5	-
$-y_{24}$	-	7.74-2	7.24-2	7.25-2	-	9.78-2	8.90-2	9.00-2	-	8.99-5	-
$-y_{14}$	-	1.94-2	1.81-2	1.60-2	-	2.03-2	1.80-2	1.60-2	-	2.26-8	-
$-y_{15}$	-	-	4.81-3	-	-	-	4.20-3	-	-	-	-

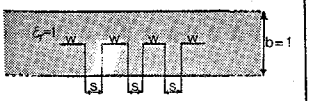

The Table values are normalized to the free space characteristic admittance

VI. CONCLUSIONS

An exact theory based on conformal mapping technique has been developed for the analysis of multiconductor striplines enclosed in a rectangular box with a homogeneous dielectric medium. Compared to methods based on lattice approximations, such as [18], the advantages are the following.

1) Explicit control of the error in the result.
2) A reduction in computer time of at least 30:1.
3) From 2) it also follows that the synthesis of characteristic immittance matrices by employing optimization algorithms is economically feasible. One important drawback of the method, which it shares with mapping techniques in general, is that inhomogeneously filled media can only be treated approximately.

The problem of synthesis has been solved for design purposes by using an efficient optimization procedure working with a repeated analysis technique.

APPENDIX

HYPERELLIPTIC MAPPING FUNCTIONS

In the mapping from Fig. 2 to Fig. 3 the following mapping function is employed:

$$z(y) = \int_{-\infty}^{y} [\prod_{m=1}^{n} (y - y_{0m}) / \prod_{m=1}^{2n+2} (y - y_m)^{1/2}] \, dy. \quad \text{(A1)}$$

From the theory of complex functions it is obvious that we are dealing with a many valued analytical integrand with $2n + 2$ branch points and with interconnecting branch cuts. However, if we make infinitesimal semicircle indentations around the branch points in the upper half-plane of Fig. 2, we can keep the path of integration in one Riemann sheet. The closure of the integration path with an infinitely large upper half-plane semicircle now guarantees the closure of the mapping in Fig. 3. This is clear from Cauchy's integral theorem, because the contributions from the integration on the semicircles around the branch points tend to zero with the radius. The real part of the Cauchy integral now shows that the width of the upper and lower conductors, k and J, are equal. Analogously, the imaginary parts guarantee the equal lengths of the side walls. Also, the number of integrals to be evaluated can be reduced by one.

Consider now the numerical integration of real definite integrals (1), where the path of integration is between two consecutive poles:

$$\int_{y_k}^{y_{k+1}} [y^{j-1} / | \prod_{m=1}^{2n+2} (y - y_m)^{1/2} |] \, dy. \quad \text{(A2)}$$

From a functional viewpoint this is a hyperelliptic integral of the first kind for $n \geq 2$ [22], and hence it can only be expressed in elliptic integrals under very rare conditions. Unfortunately, the theory of hyperelliptic functions of today is rather undeveloped, and this applies also to a certain degree to their numerical evaluation. In this work a newly derived analytic method will be used in connection with very fast quadrature algorithms [23]. Consider an improper integral with singularities at both endpoints:

$$I = \int_a^b \frac{f(x)}{(x-a)^\alpha (b-x)^\beta} \, dx, \qquad (0 < (\alpha,\beta) < 1). \quad \text{(A3)}$$

If we can extract the singular terms of the integral we are left with a well-behaving function with *removable* singularities. This is often an easy matter. Thus

$$I = I_1 + I_2 + I_3 \quad \text{(A4)}$$

where

$$I_1 = \int_a^b \left\{ \frac{f(x)}{(x-a)^\alpha (b-x)^\beta} - \frac{A_0}{(x-a)^\alpha} - \frac{B_0}{(b-x)^\beta} \right\} dx \quad \text{(A5.1)}$$

$$I_2 = \int_a^b A_0(x-a)^{-\alpha}\,dx = \frac{A_0}{1-\alpha}(b-a)^{1-\alpha} \qquad \text{(A5.2)}$$

$$I_3 = \int_a^b B_0(b-x)^{-\beta}\,dx = \frac{B_0}{1-\beta}(b-a)^{1-\beta}. \qquad \text{(A5.3)}$$

Now the evaluation of (A5.1) can be performed with any available quadrature scheme observing the value of the integrand at the endpoints: $-B_0(b-a)^{-\beta}$ and $-A_0(b-a)^{-\alpha}$, respectively. Very satisfactory results have been achieved using automatic quadrature schemes with the specified numerical error controlling the number of subdivisions of the integration interval [24].

ACKNOWLEDGMENT

The constant encouragement of Prof. E. F. Bolinder during this work has been of great value, as has the typing and drawing work of Ms. C. Eliasson.

REFERENCES

[1] K. G. Black and T. J. Higgins, "Rigorous determination of the parameters of microstrip transmission lines," *IRE Trans. Microwave Theory Tech. (Special Issue on the Symposium on Microwave Strip Circuits)*, vol. MTT-3, pp. 93–113, Mar. 1955.

[2] R. Pregla, "Calculation of the distributed capacitances and phase velocities in coupled microstrip lines by conformal mapping techniques," *Arch. Elek. Übertragung*, vol. 26, pp. 470–474, Nov. 1972.

[3] W. Magnus and F. Oberhettinger, "Die Berechnung des Wellenwiderstandes einer Bandleitung mit Kreisförmigem bzw. Rechteckigem Aussenleiterquerschnitt," *Arch. Elektrotech.*, vol. 37, pp. 380–390, Mar. 1943.

[4] S. B. Cohn, "Characteristic impedance of the shielded-strip transmission line," *IRE Trans. Microwave Theory Tech.*, vol. MTT-2, pp. 52–57, July 1954.

[5] R. H. T. Bates, "The characteristic impedance of the shielded slab line," *IRE Trans. Microwave Theory Tech.*, vol. MTT-4, pp. 28–33, Jan. 1956.

[6] J. D. Morgan, "Coupled strip transmission lines with rectangular inner conductors," *IRE Trans. Microwave Theory Tech.*, vol. MTT-5, pp. 92–99, Apr. 1957.

[7] H. J. Riblet, "The exact dimensions of a family of rectangular coaxial lines with given impedance," *IEEE Trans. Microwave Theory Tech.*, vol. MTT-20, pp. 538–541, Aug. 1972.

[8] R. Ekinge, "Microwave TEM-mode power dividers and couplers," Ph.D. dissertation, School Elec. Eng., Chalmers Univ. Technol., Gothenburg, Sweden, Tech. Rep. 15, pp. 4–22, Apr. 1972.

[9] R. Sato and R. Ikeda, "Line constants," in *Advances in Microwaves: Microwave Filters and Circuits*, A. Matsumoto, Ed. New York: Academic, 1970, pp. 123–156.

[10] S. B. Cohn, "Shielded coupled-strip transmission line," *IRE Trans. Microwave Theory Tech.*, vol. MTT-3, pp. 29–38, Oct. 1955.

[11] J. Ishi, "The characteristic impedance of unsymmetric coupled strip transmission line" (in Japanese), presented at the Nat. Meeting Institute of Electronic Communication Engineers (Japan), 1959.

[12] T. Ikeda and R. Sato, "The characteristic impedance of unsymmetric coupled transmission line" (in Japanese), presented at the Joint Meeting Institute of Electrical Engineers of the Tohoku District, 1963.

[13] T. Ikeda, N. Saito, R. Sato, and K. Nagai, "The characteristic impedance of unsymmetric coupled transmission line" (in Japanese), in *Rec. Electron. Commun. Eng.*, vol. 32, no. 2, 1963, pp. 13–16.

[14] K. Itakura, S. Yamamoto, and T. Azakami, "Coupled strip transmission line with three center conductors" (in Japanese), presented at the 1965 Microwave Transmission System Conf., Institute of Electronic Communication Engineers (Japan).

[15] V. E. Dunn, "Realization of microwave pulse compression filters by means of folded-tape meander lines," Stanford Electron. Lab., Stanford, Calif., SEL-62-113 (TR 557-3), Oct. 1962.

[16] E. L. Kollberg, "Conductor admittance in transverse TEM filters and slow-wave structures," *Electron. Lett.*, vol. 3, pp. 294–296, July 1967.

[17] R. Pregla, "Distributed capacitances for coupled rectangular bars of finite width," *Arch. Elek. Übertragung*, vol. 25, pp. 69–72, Feb. 1971.

[18] B. Lennartsson, "A network analogue method for computing the TEM characteristics of planar transmission lines," *IEEE Trans. Microwave Theory Tech.*, vol. MTT-20, pp. 586–591, Sept. 1972.

[19] L. J. P. Linnér, "Explicit expressions for the geometric dimension of symmetrical coupled striplines," *Electron. Lett.*, vol. 10, pp. 45–46, Feb. 1974.

[20] F. Tricomi, *Elliptische Funktionen*. Leipzig, Germany: Akademische Verlags-gessellschaft, 1948.

[21] M. J. D. Powell, "A hybrid method for nonlinear equations," in *Numerical Methods for Nonlinear Algebraic Equations*, P. Rabinowitz, Ed. London, England: Gordon and Breach, 1970.

[22] P. F. Byrd and M. D. Friedman, *Handbook of Elliptic Integrals for Engineers and Scientists*. Berlin, Germany: Springer, 1971, pp. 252–256.

[23] L. J. P. Linnér, "Solving improper integrals by the extraction of singular terms," Div. Network Theory, Chalmers Univ. Technol., Gothenburg, Sweden, Rep. TR 7302, Apr. 1973.

[24] J. W. Lyness, "Algorithm 379, SQUANK: Simpson quadrature used adaptively—noise killed," *Commun. Ass. Comput. Mach.*, vol. 13, pp. 260–263, Apr. 1970.